A state space representation model for parasitic losses in MIMO capacitive wireless power systems

A State Space Representation Model for Parasitic Losses in MIMO Capacitive Wireless Power Systems

Aris van Ieperen
Cosys-Lab
University of Antwerp
Antwerp, Belgium
aris.vanieperen@uantwerpen.be

Stijn Derammelaere
Cosys-Lab
University of Antwerp
Antwerp, Belgium
AnSyMo/Cosys
Flanders Make
Belgium
stijn.derammelaere@uantwerpen.be

Ben Minnaert
Cosys-Lab
University of Antwerp
Antwerp, Belgium
ben.minnaert@uantwerpen.be

***Abstract*—Generally, an idealized equivalent circuit is used to model capacitive wireless power transfer, ignoring equivalent series resistances. However, given the picofarad range of electric coupling, more detailed models that include these non-idealities are required. Unfortunately, taking into account parasitic effects can result in rising calculation complexity, in particular for a capacitive wireless power transfer system with multiple transmitters and multiple receivers, i.e., a Multiple Input – Multiple Output configuration. In this work, a model based on state space representation is applied to allow easy calculation of the optimal operating state, i.e. maximizing efficiency or power output. The model is applied to an illustrative example of capacitive wireless power transfer with multiple transmitters and receivers, highlighting the differences between the idealized and non-ideal equivalent circuit representation.**

***Index Terms*—wireless power, resonance, state space**

I. Introduction

Capacitive wireless power transfer (CPT) allows for the transfer of energy from one or more transmitters to one or more receivers without the need for a physical connection. Contrary to the well-known inductive wireless power transfer that uses the magnetic field to transfer power wirelessly, CPT applies the electric field as medium. Depending on the distance between transmitter(s) and receiver(s), and their relative (lateral and/or rotational) alignment, the performance of the energy transfer varies. This implies that every time a receiver is wirelessly coupled to a transmitter, the coupling between them differs, which changes the optimal working point. By applying variable impedance compensation, the system can be kept at its optimal working point, regardless of the value of the unpredictable coupling.

The current literature that describes how to find these optimum compensation networks for CPT (e.g., [1], [2]) have introduced idealizations within their models, e.g., ignoring parasitic impedances of capacitors and coils. One of the main reasons for this idealization, is the rising complexity of non-ideal systems, in particular for a setup with multiple transmitters and multiple receivers, i.e., a Multiple Input – Multiple Output (MIMO) configurations. These idealizations are appropriate for inductive wireless systems, but given the picofarad range of CPT coupling, more detailed models, including non-idealities are a prerequisite.

In this work, a model based on state space representation is applied to allow easy calculation of the optimal operating state, applicable to either optimizing efficiency or maximizing power output. The model is applied to an illustrative MIMO CPT example, highlighting the differences between the idealized and non-ideal equivalent circuit representation.

II. Methodology

A. Stace Space Representation

Using the state space representation [3]–[6], the system can be described as a set of first-order differential equations in a concise mathematical notation by the use of vector equations. This state space representation is applicable to both linear and non-linear systems, is applicable to MIMO systems, and is straightforward to solve numerically.

In Fig. 1, a schematic overview of an M by N MIMO CPT system is shown. The desired coupling between each transmitter capacitor C_i and receiver capacitor C_j, where i is the number of the transmitter and j the number of the receiver plus the total number of transmitters, is represented by the gray arrows. The red arrows represent the undesired coupling between different transmitters and receivers.

In Fig. 2, the equivalent circuit of a single transmitter and receiver is shown. Each transmitter is driven by the current source I_i. The shunt resistor R_i is used to describe the losses in the circuit. The inductors L_i are used to create a resonant scheme by using an inductance of $1/\omega_0^2 C_i$ with ω_0 the operating angular frequency of the current source I_i. The resistors R_{L_i} and R_{C_i} represent the inductor's and

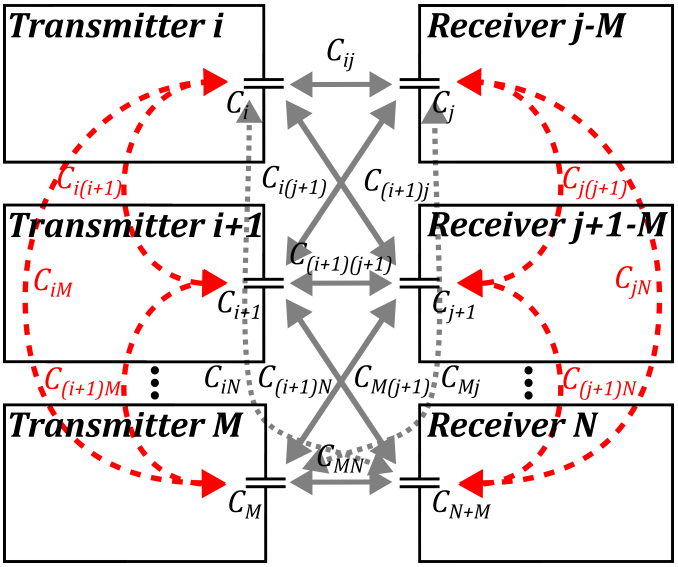

Fig. 1. Schematic overview of an M by N MIMO system.

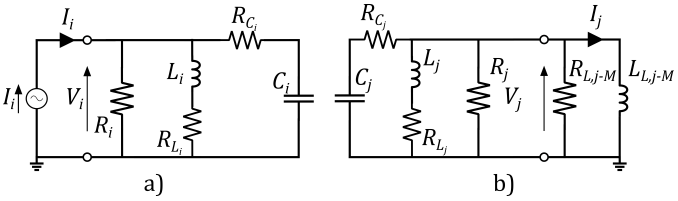

Fig. 2. Schematic overview of a) the transmitter and b) the receiver.

capacitor's equivalent series resistance (ESR) respectively. In CPT literature, these resistors are often neglected, i.e., equal zero in the idealized equivalent circuit. The circuit of the receiver is similar to the circuit of the transmitter, however, it does not have a current source but has a load resistance $R_{L,j-M}$ and load inductance $L_{L,j-M}$.

We introduce the capacitor voltages and the inductor currents as the state variables $\mathbf{x}$:

$$\mathbf{x} = \begin{Bmatrix} v_{C_1} \\ \vdots \\ v_{C_{M+N}} \\ i_{L_1} \\ \vdots \\ i_{L_{M+N}} \\ i_{L_{L_1}} \\ \vdots \\ i_{L_{L_N}} \end{Bmatrix}, \tag{1}$$

and the current sources as inputs $\mathbf{u}$:

$$\mathbf{u} = \begin{Bmatrix} i_{I_1} \\ \vdots \\ i_{I_M} \end{Bmatrix}. \tag{2}$$

Using the capacitor current equation

$$i_C = C\frac{dv_C}{dt} \tag{3}$$

and inductor voltage equation

$$v_L = L\frac{di_L}{dt}, \tag{4}$$

the system can be described as a system of first-order derivative equations of the state variables. Using Kirchhoff's voltage and current law, expressions for i_C and v_L can be found.

The current through the coupling capacitances $i_{C_{ij}}$ is described as a function of the change in voltage of the other capacitances following:

$$i_{C_{ij}} = C_{ij}\frac{dv_{C_i}}{dt} - C_{ij}\frac{dv_{C_j}}{dt}. \tag{5}$$

For the transmitter shown in Fig. 2a, the capacitor current i_{C_i} is given by:

$$i_{C_i} = i_{I_i} - i_{R_i} - i_{L_i} - i_{C_{ik}} \tag{6}$$

with $k = \{n \in \mathbb{Z}^+ \mid n \leq M+N, \forall\, n \neq i\}$.

Using (5), the current through the coupling capacitors $i_{C_{ik}}$ can be expressed as first-order derivatives of the state variables. Therefore we only need to find a different expression for the current through the resistor i_{R_i}. We can express this current as:

$$i_{R_i} = \frac{v_i}{R_i}, \tag{7}$$

with the input voltage v_i equal to:

$$v_i = v_{C_i} + i_{R_{C_i}}R_{C_i} = v_{C_i} + (i_{C_i} + i_{C_{ik}})R_{C_i}. \tag{8}$$

Substitution of (7) and (8) in (6) results in the following expression of the capacitor current:

$$i_{C_i} = \frac{i_{I_i} - \frac{v_{C_i}}{R_i} - i_{L_i} - (1 + \frac{R_{C_i}}{R_i})i_{C_{ik}}}{1 + \frac{R_{C_i}}{R_i}}. \tag{9}$$

The voltage over the inductor for the transmitter shown in Fig. 2a, v_{L_i}, is given by:

$$v_{L_i} = v_i - i_{L_i}R_{L_i}. \tag{10}$$

Here, the current through the inductor i_{L_i} is a state variable and the inductor's ESR R_{L_i} is a constant. Therefore, we only need to find a different expression for the input voltage v_i.

Using the expression of v_i as derived in (8) and express the current through the capacitor's ESR resistor $i_{R_{C_i}}$ as:

$$i_{R_{C_i}} = i_{I_i} - \frac{v_i}{R_i} - i_{L_i}, \tag{11}$$

we can write v_i as

$$v_i = \frac{v_{C_i} + (i_{I_i} - i_{L_i})R_{C_i}}{1 + \frac{R_{C_i}}{R_i}}, \tag{12}$$

which only contains constants, inputs, and state variables. Substitution of (12) in (10) results into:

$$v_{L_i} = \frac{v_{C_i} + (i_{I_i} - i_{L_i})R_{C_i}}{1 + \frac{R_{C_i}}{R_i}} - I_{L_i}R_{L_i}. \tag{13}$$

For the receiver shown in Fig. 2b, the capacitor current is given by:

$$i_{C_j} = i_{C_{jk}} - i_{L_j} - i_{R_j} - i_{R_{L,j-N}} - i_{L_{L,j-N}}. \tag{14}$$

As the inductor currents i_{L_j} and $i_{L_{L,j-N}}$ are state variables, and the current through the coupling capacitances can be expressed as first-order derivatives of the state variables using (5), we only need to find new expressions for the currents through the resistors i_{R_j} and $i_{R_{L,j-N}}$.

The current through the resistor i_{R_j} can be expressed as:

$$i_{R_j} = \frac{v_j}{R_j}, \tag{15}$$

and the current through the inductor's ESR resistor $i_{R_{L,j-N}}$ can be expressed as:

$$i_{R_{L,j-N}} = \frac{v_j}{R_{L,j-N}}. \tag{16}$$

In these equations, the output voltage v_j is equal to

$$v_j = v_{C_j} - i_{R_{C_j}}R_{C_j}, \tag{17}$$

where the current through the capacitor's ESR resistor $i_{R_{C_j}}$ is equal to

$$i_{R_{C_j}} = i_{C_{jk}} - i_{C_j}. \tag{18}$$

Substitution of (15), (16), (17) and (18) in (14) results in:

$$i_{C_j} = \frac{(1 + \frac{R_{C_j}}{R_j} + \frac{R_{L,j-N}}{R_j})i_{C_{jk}} - i_{L_j} - i_{L_{L,j-N}}}{1 + \frac{R_{C_j}}{R_j} + \frac{R_{L,j-N}}{R_j}}. \tag{19}$$

For the voltage over the inductor v_{L_j} in the receiver as shown in Fig. 2b, we get:

$$v_{L_j} = v_j - i_{L_j}R_{L_j}. \tag{20}$$

We can express the current through the capacitor's ESR resistor $i_{R_{C_j}}$ as:

$$i_{R_{C_j}} = i_{L_j} + \frac{v_j}{R_j} + \frac{v_j}{R_{L,j-N}} + i_{L_{L,j-N}}, \tag{21}$$

and we can express the output voltage v_j as:

$$v_j = \frac{v_{C_j} - (i_{L_j} + i_{L_{L,j-N}})R_{C_j}}{1 + \frac{R_{C_j}}{R_j} + \frac{R_{C_j}}{R_{L,j-N}}}. \tag{22}$$

Substitution of (22) in (20) gives:

$$v_{L_j} = \frac{v_{C_j} - (i_{L_i} + i_{L_{L,j-N}})R_{C_i}}{1 + \frac{R_{C_j}}{R_j} + \frac{R_{C_j}}{R_{L,j-N}}} - I_{L_j}R_{L_j}. \tag{23}$$

The expression of the voltage over the output inductor $v_{L_{L,j-N}}$ is equal to the output voltage v_j, as defined in (22).

By applying equation (3) to the derived expressions for the capacitor currents and inductor voltages in (9), (13), (19), (22), and (23), we get the desired set of first-order derivative equations of the state variables.

Considering the input and output voltages v_i and v_j respectively as outputs, we can use the expressions in (12) and (22) to define the output equations. As the set of first-order derivative equations and output equations are a function of constants, the state variables, and the inputs, we can take out the state variables and inputs in these equations and write the system in the standard state space form as:

$$\begin{aligned} \frac{d}{dt}\mathbf{x} &= \mathbf{A}\mathbf{x} + \mathbf{B}\mathbf{u} \\ \mathbf{y} &= \mathbf{C}\mathbf{x} + \mathbf{D}\mathbf{u}, \end{aligned} \tag{24}$$

with $\mathbf{A}$ the system matrix, $\mathbf{B}$ the input matrix, $\mathbf{C}$ the output matrix and $\mathbf{D}$ the feed-through matrix.

Using the system model given in (24), the transfer functions of the inputs $\mathbf{u}$ to the outputs $\mathbf{y}$ can be calculated using:

$$P(s) = \frac{\mathbf{y}}{\mathbf{u}} = \mathbf{C}(s\mathbf{I} - \mathbf{A})^{-1}\mathbf{B} + \mathbf{D}, \tag{25}$$

with s the Laplace variable.

For a given frequency, these transfer functions give for each input I_i to each output V_i, V_j the magnitude and phase. By adding the contribution of each input to one of the outputs, the total magnitude and phase Φ_{V_i} of each output can be calculated. The input power P_{in} is given by the sum of the power of all input ports:

$$P_{in} = \sum_{i=1}^{M} \frac{V_i I_i}{\sqrt{2}} \cos(\Phi_{V_i}), \tag{26}$$

and the output power P_{out} is given by the sum of the power of each output port, which can be calculated using the magnitude of the output voltages V_j and the resistance of output resistor $R_{L,j-M}$:

$$P_{out} = \sum_{j=1}^{N} \frac{\left(\frac{V_j}{\sqrt{2}}\right)^2}{R_{L,j-M}}. \tag{27}$$

The efficiency η of the system is then given by:

$$\eta = \frac{P_{in}}{P_{out}}. \tag{28}$$

B. Numerical Optimization

The transfer functions are obtained with symbolic expressions for the output impedance, allowing for fast computation of the resulting input and output voltages needed to calculate the output power and efficiency as defined in (27) and (28). The optimal values for the output impedance for the maximum power transfer and maximum efficiency are found by numerical optimization, utilizing the MATLAB® optimization toolbox.

C. Typical ESR Values

In order to implement the parasitic resistances into the model, typical values for CPT are required.

Capacitive couplers can either use air or a dielectric material as transfer medium. The benefit of using a dielectric material is that the coupling capacitance can be increased, however, this will come at the cost of a higher resistive part due to larger dielectric losses. These dielectric losses between couplers are neglected when using air as medium, however, [7] reports the dielectric losses in commonly used materials to be at a negligible level as well.

Only few studies report measured ESR values of CPT couplers. A measured ESR of $1.2\,\Omega$ for a capacitive coupler with a coupling capacitance of $96\,\mathrm{pF}$ using air as dielectric medium at $300\,\mathrm{kHz}$ is found in [8]. A measured ESR of $5.1\,\Omega$ for a capacitive coupler with a coupling capacitance of $13.9\,\mathrm{nF}$ using lead zirconate titanate as dielectric medium at $217\,\mathrm{kHz}$ is found in [9].

A measured ESR of $0.5\,\Omega$ is reported in [8] for a $39\,\mu\mathrm{H}$ air core inductor at a frequency of $300\,\mathrm{kHz}$. The ESR of commercially available air core inductors can also be found in the manufacturer's datasheet, such as the 132-18SM from Coilcraft, which has a reported ESR of $0.442\,\Omega$ for a $422\,\mathrm{nH}$ air core inductor at $10\,\mathrm{MHz}$.

III. Results and Discussion

To investigate the influence of the ESR on the optimal working point in a MIMO CPT system, the system as proposed in [2] is extended with inductor and capacitor ESR. It consists of a MIMO CPT system with 2 transmitters and 3 receivers. The parameter values of this system can be found in Tab. I.

TABLE I
Parameter values.

Parameter	Value	Unit	Parameter	Value	Unit
C_1	350	pF	f	10	MHz
C_2	300	pF	I_1	100	mA
C_3	250	pF	I_2	200	mA
C_4	225	pF	L_1	724	nH
C_5	200	pF	L_2	844	nH
C_{12}	30.00	pF	L_3	1013	nH
C_{13}	75.00	pF	L_4	1126	nH
C_{14}	56.25	pF	L_5	1267	nH
C_{15}	40.00	pF	R_1	1000	Ω
C_{23}	62.50	pF	R_2	800	Ω
C_{24}	45.00	pF	R_3	667	Ω
C_{25}	40.00	pF	R_4	571	Ω
C_{34}	11.25	pF	R_5	500	Ω
C_{35}	4.00	pF			
C_{45}	10.00	pF			

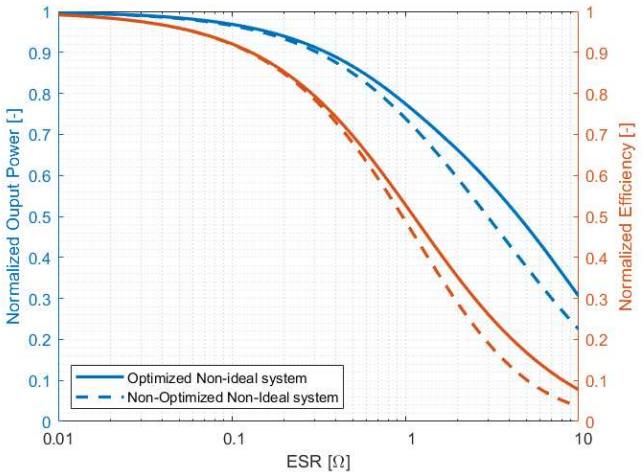

Fig. 3. Normalized output power and efficiency as a function of the ESR for the non-ideal optimal system (solid line) and the non-ideal, non-optimized system (dashed line).

The normalized output power and efficiency as function of the ESR are shown in Fig. 3. We consider two configurations: (i) the CPT system where the terminations are optimized for the ideal (zero ESR) scenario and (ii) the system where at each data point, an impedance compensation variation is performed to realize the optimal working point in function of the ESR value.

As expected, the maximum output power and efficiency decrease for higher ESR values. The difference between the non-optimized and optimized system gets larger as well for increasing ESR. Regarding the output power, a deviation of $5\,\%$ between both configurations occurs at an ESR value of $0.75\,\Omega$. At this point, the maximum power of the system is $60\,\%$ of the maximum power of the ideal system with no ESR taken into account, meaning a significant influence of the ESR at this point. Regarding the efficiency, a $5\,\%$ deviation occurs at an ESR value of $1.15\,\Omega$. The maximum efficiency of the non-ideal system at this point is $75\,\%$ of the maximum efficiency, also indicating a significant influence of the ESR at this point. Notice that these ESR values are in line with typical values for inductor and capacitor coupling.

The output power and efficiency are a function of the load termination. In Figs. 4 and 5, the normalized output power and efficiency as a function of the load resistance are shown for both the ideal and the non-ideal system with an ESR value for both the inductor and capacitor of $1\,\Omega$. For each line, one of the load resistances is varied while the others are kept at their optimal value. The values for the illustrative MIMO examples were chosen such that both a low (e.g., load $R_{L,3}$) and high (e.g., load $R_{L,1}$) dependence on the load termination are present.

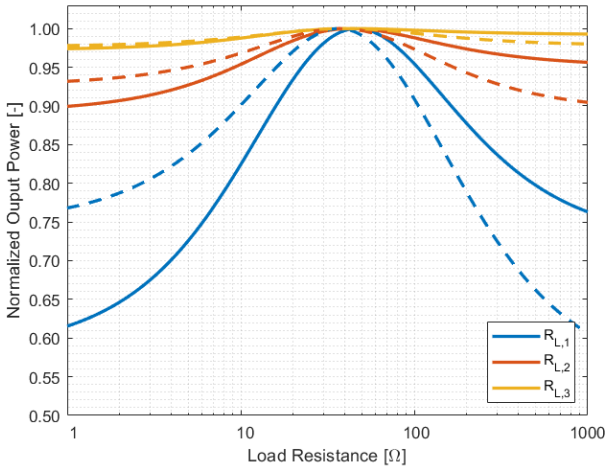

Fig. 4. Normalized output power as a function of the load resistance for the ideal system (solid line) and non-ideal system with ESR values of 1 Ω (dashed line).

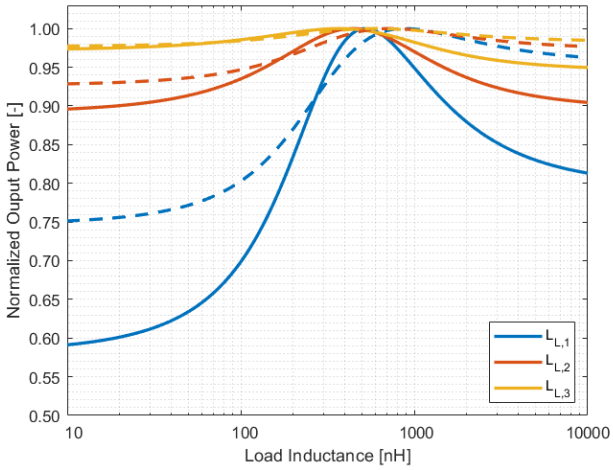

Fig. 6. Normalized output power as a function of the load inductance for the ideal system (solid line) and non-ideal system with ESR values of 1 Ω (dashed line).

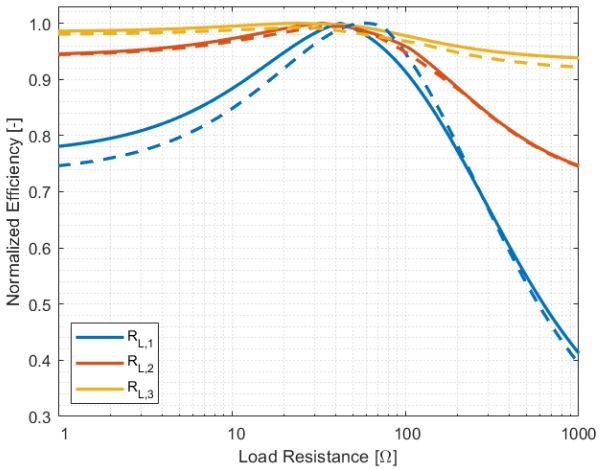

Fig. 5. Normalized efficiency as a function of the load resistance for the ideal system (solid line) and non-ideal system with ESR values of 1 Ω (dashed line).

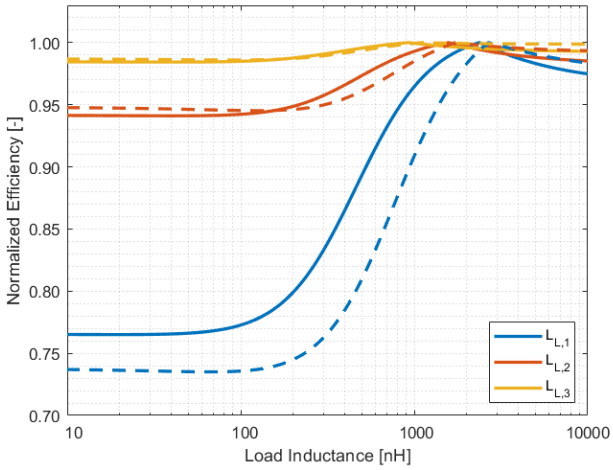

Fig. 7. Normalized efficiency as a function of the load inductance for the ideal system (solid line) and non-ideal system with ESR values of 1 Ω (dashed line).

It can be noted that the effect of varying one of the load resistances from its optimal value has a similar effect for both the ideal and non-ideal system. For the output power, the optimal load resistances for the non-ideal system are smaller than the optimal load resistances of the ideal system. The loss in performance by using an output resistance smaller than the optimal value is less for the non-ideal system compared to the loss in performance for the ideal system, whereas, by using an output resistance larger than the optimal value the loss in performance is larger for the non-ideal system. For the efficiency, the optimal load resistances for the non-ideal system are larger than the optimal load resistances of the ideal system. For load resistances smaller than the optimal value, the effect on the efficiency is slightly larger for the non-ideal system. For load resistances larger than the optimal value, the effect on the efficiency is similar for both the non-ideal and the ideal system.

In Figs. 6 and 7, the normalized output power and efficiency as a function of the load inductance are shown for both the ideal and the non-ideal system with an ESR value for both the inductor and capacitor of 1 Ω. For each line, one of the load inductances is varied while the others are kept at their optimal value. For the output power, the effect of varying the inductances from their optimal value is smaller for the non-optimal system, and is especially small for inductances larger than the optimal values. This is also the case for the efficiency, however, it should be noted that here it is the case for both the ideal and the non-ideal system. For inductances smaller than their optimal values, the difference in efficiency loss is small.

IV. Conclusion

A state space approach of analyzing an N+M-sized MIMO CPT system with inductor and capacitor ESR is presented. A case study has been performed using a 2-input, 3-output CPT system to investigate the effect of the ESR on the optimal point. It was shown that the model can easily determine the resistive and reactive load terminations to maximize either power output or efficiency. Moreover, for typical inductor and capacitor values of ESR, there is a non-negligible effect of the parasitic losses on the optimal working point, indicating the need to include non-idealities into the equivalent circuit of CPT.

References

[1] M. Dionigi, M. Mongiardo, G. Monti, and R. Perfetti, "Modelling of wireless power transfer links based on capacitive coupling," *International Journal of Numerical Modelling: Electronic Networks, Devices and Fields*, vol. 30, no. 3-4, p. e2187, 2017.

[2] B. Minnaert, G. Monti, A. Costanzo, and M. Mongiardo, "Power maximization for a multiport network described by the admittance matrix," *URSI Radio Science Letters*, vol. 2, 2021.

[3] A. K. Swain, M. J. Neath, U. K. Madawala, and D. J. Thrimawithana, "A dynamic multivariable state-space model for bidirectional inductive power transfer systems," *IEEE Transactions on Power Electronics*, vol. 27, pp. 4772–4780, 2012.

[4] T. Tan, K. Chen, Y. Jiang, Z. Zhao, and L. Yuan, "Dynamic modeling and analysis of multi-receiver wireless power transfer system." Institute of Electrical and Electronics Engineers Inc., 6 2019, pp. 391–395.

[5] Y. Chen, S. Dong, B. Wei, B. Zhang, H. Ma, and C. Zhu, "Research on GSSA model of wireless power transfer system using a quasi z-source converter." Institute of Electrical and Electronics Engineers Inc., 2022, pp. 1876–1881.

[6] Y. Awadh and S. Saat, "State feedback controller design for capacitive power transfer system." Institute of Electrical and Electronics Engineers Inc., 7 2021.

[7] S. Zang, Q. Zhu, and A. P. Hu, "Basic analysis of coupler loss in capacitive power transfer systems." Institute of Electrical and Electronics Engineers Inc., 2022, pp. 15–20.

[8] C. Suarez, M. Kalmes, J. Suffeleers, and W. Martinez, "Frequency splitting in an LCLC capacitive wireless power transfer system for electric vehicle charging," vol. 2020-October. IEEE Computer Society, 10 2020, pp. 3622–3627.

[9] A. P. Hu, C. Liu, and H. L. Li, "A novel contactless battery charging system for soccer playing robot," 2008, pp. 646–650.